

Reflection by defects in a tight-binding model of nanotubes

T. Kostyrko

*Solid State Division, Oak Ridge National Laboratory, Oak Ridge, Tennessee 37831-6030
and Institute of Physics, Adam Mickiewicz University, ul. Umultowska 85, 61-614 Poznań, Poland*

M. Bartkowiak

*Solid State Division, Oak Ridge National Laboratory, Oak Ridge, Tennessee 37831-6030;
Department of Physics and Astronomy, University of Tennessee, Knoxville, Tennessee 37996-1200;
and Institute of Physics, Adam Mickiewicz University, ul. Umultowska 85, 61-614 Poznań, Poland*

G. D. Mahan

*Solid State Division, Oak Ridge National Laboratory, Oak Ridge, Tennessee 37831-6030
and Department of Physics and Astronomy, University of Tennessee, Knoxville, Tennessee 37996-1200*

(Received 8 June 1998; revised manuscript received 3 August 1998)

We use a transfer-matrix method to study defects in a tight-binding model of carbon nanotubes. We calculate the reflection coefficient R for a simple barrier created by a pointlike defect of strength E in armchair (N_a, N_a) and zigzag ($N_a, 0$) nanotubes for the whole range of energy ω and arbitrary number of conducting channels. We find that R scales at the Fermi level (i.e., $\omega = 0$) as $R = s(E/t)^2/N_a^2$ (t being the hopping parameter), where $s \approx 1/6$ (for the armchair nanotubes) and $s \approx 1/2$ (for the zigzag nanotubes). We also perform a similar calculation for a “5-77-5” defect and find the results to be like the ones obtained for a strong point defect with $E = 6t$. [S0556-2821(98)05114-5]

I. INTRODUCTION

An individual single-wall carbon nanotube (SWCNT) represents a strictly one-dimensional (1D) system with a great number of carbon atoms in the unit cell of the 1D Bravais lattice (for a review see Refs. 1 and 2). In the 1D systems the electron wave functions are known to be localized in the presence of disorder and transport properties of such a system is determined by hopping between the localized levels. With an increase of the tube radius, the system becomes more and more similar to an infinite graphite plane, i.e., 2D system. The role of disorder decreases and the states may be treated as extended, at least on the scale length of the realistic nanotube length. Recent experimental observations of a single-electron tunneling through discrete electronic levels in an individual SWCNT show the electron states to be extended over a distance as large as $3 \mu\text{m}$ (Ref. 3). On the other hand, various kinds of defect are known to be present in rolled up graphene sheet of the carbon nanotubes,⁴⁻⁶ however their influence on electronic and transport properties of these systems is poorly known. The purpose of our paper is to understand how these properties may be related to a particular defect type, nanotube radius, and its helicity.

In particular, we study here the reflection from a barrier created by defects that may appear in the SWCNT. We also calculate the changes in the density of states introduced by a single defect and show how these changes can be related to the reflection of an incident electron for arbitrary number of the conducting channels. We analyze the results as a function of the defect strength and nanotube radius and determine simple asymptotic formulas for the reflection from the studied defects which should prove useful in estimations of the conductance.

Recent theoretical works on the role of defects in SWCNT concerned mainly a defect present at the junction of two nanotubes of different helicity^{7,9} and were concentrated on calculations of the local electron density of states close to the junctions. Chico *et al.*,⁸ using a “Green-function matching method,” studied also the conductance for a single vacancy, which they simulated as an extremely strong point defect with nearby bonds interrupted. They did not discuss their data as a function of the defect strength, however, and did not mention a possible scaling laws of the conductance as a function of defect strength and nanotube radius. A related work was performed by Tamura and Tsukada¹⁰ who studied the transmission through a barrier created at model junctions. They determined the scaling law for the conductance at the Fermi energy in terms of the ratio of the radii of the nanotubes at the junctions and the junctions’ lengths. Our approach is also more general than that in Ref. 10 in that it allows one to study the conductance for the whole energy range, including an arbitrary number of conducting channels.

II. GENERAL FORMULATION

We assume that the standard model for the energy bands of graphite can be applied to nanotubes. The principal conduction and valence bands are composed of p_z orbitals. Band-structure calculation¹¹ show that the nearest-neighbors tight-binding model gives an adequate description. So far all physical measurements on nanotubes indicate they are Fermi liquids rather than Luttinger liquids. Thus, we adopt the model that the electrons are ordinary quasiparticles described by a tight-binding model, which occasionally scatter from impurities,

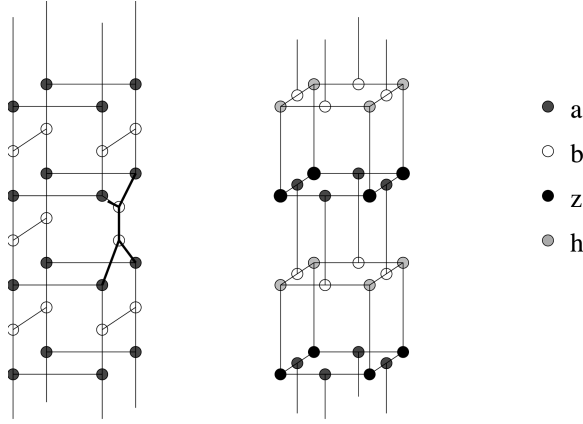


FIG. 1. The schematic picture of (2,2) armchair and (4,0) zigzag nanotubes, showing division into unit cells. In the (2,2) nanotube a 5-7-7-5 defect is shown with heavy lines.

$$\mathcal{H} = \sum_j [a_{j+1}^\dagger t_j b_j + b_j^\dagger t_j^\dagger a_{j+1} + a_j^\dagger H_j^a a_j + b_j^\dagger H_j^b b_j + a_j^\dagger W_j b_j + b_j^\dagger W_j^\dagger a_j] \quad (1)$$

where a_j, b_j denote n_b -component electron operators for the a and b orbitals of j th cell (see Fig. 1). The first two terms in Eq. (1) describe electron hopping between neighboring cells, and t_j is a matrix of the corresponding hopping parameters. The next two terms, including Hermitian matrices $H_j^{a,b}$, describe intracell hopping processes as well as interaction with on site impurities. The last two terms describe intracell hopping between a and b orbitals. In zigzag nanotubes, in addition to a and b orbitals one can have orbitals not connected directly to either of the neighboring cells. They can be eliminated at a later stage of the theory at the cost of modifying the intracell hopping matrix W_j .

The standard method to study effects of disorder in a one-band 1D system is a transfer-matrix method (for a review see Ref. 12). From the transfer matrix one can calculate density of states, transmission coefficients, and (using the latter) electrical conductivity of the finite 1D system at $T=0$ K.^{13,14} Application of this method to a many band system was discussed recently by Molinari,¹⁵ and we follow the formalism presented there (see also Ref. 16 for a review).

For a given energy ω , using the Schrödinger equation with the Hamiltonian (1) and the wave function

$$\Psi = e^{-i\omega t} \sum_j (\alpha_j a_j^\dagger + \beta_j b_j^\dagger) |0\rangle \quad (2)$$

leads to a system of recurrence equations for the coefficient vectors α and β :

$$A_j \alpha_j + t_{j-1} \beta_{j-1} + W_j \beta_j = 0, \quad A_j = H_j^a - \omega I, \quad (3)$$

$$B_j \beta_j + t_j^\dagger \alpha_{j+1} + W_j^\dagger \alpha_j = 0, \quad B_j = H_j^b - \omega I, \quad (4)$$

where I denotes the unit matrix. They can be written in the form

$$\begin{pmatrix} \alpha_{j+1} \\ \beta_j \end{pmatrix} = T_j \begin{pmatrix} \alpha_j \\ \beta_{j-1} \end{pmatrix},$$

$$T_j = \begin{pmatrix} t_j^{-1\dagger} B_j W_j^{-1} A_j - t_j^{-1\dagger} W_j^\dagger & t_j^{-1\dagger} B_j W_j^{-1} t_{j-1} \\ -W_j^{-1} A_j & -W_j^{-1} t_{j-1} \end{pmatrix}, \quad (5)$$

where a transfer matrix T_j was introduced. The current in this state takes a form

$$iJ_j = \alpha_{j+1}^\dagger t_j \beta_j - \beta_j^\dagger t_j^\dagger \alpha_{j+1} \quad (6)$$

and, as follows from the fact that A_j and B_j are Hermitian, is independent of the site index j .

It is convenient to introduce the diagonal representation of the transfer matrix T for a perfect lattice site:

$$T_D = \begin{pmatrix} \Lambda & \mathbf{0} \\ \mathbf{0} & \tilde{\Lambda} \end{pmatrix} = S_T^{-1} T S_T, \quad \Lambda \tilde{\Lambda} = I, \quad (7)$$

where S_T defines the similarity transformation diagonalizing T . Using S_T , the current conservation law for a perfect lattice site can be written as

$$T_D^\dagger S_T^\dagger \begin{pmatrix} \mathbf{0} & t \\ -t^\dagger & \mathbf{0} \end{pmatrix} S_T T_D = S_T^\dagger \begin{pmatrix} \mathbf{0} & t \\ -t^\dagger & \mathbf{0} \end{pmatrix} S_T = \begin{pmatrix} V & -\gamma \\ \gamma^\dagger & \tilde{V} \end{pmatrix}, \quad (8)$$

where in the last equation we introduced a ‘‘velocity matrix’’ V , after Ref. 15.

Here we are concerned with a problem of scattering of the electron by a barrier in the system, which is otherwise perfectly periodic (by ‘‘barrier’’ we mean a finite sequence of unit cells including defects). The particle incident at the barrier splits into two parts. The amplitude of the reflected part is determined by the reflection matrix \mathcal{R} . The transmitted part, the amplitude of which is determined by the transmission matrix \mathcal{T} , cannot include an exponentially growing contributions as well as those that correspond to the wave running towards the barrier. These contributions have to be eliminated. Comparing the current, Eq. (6), on the two sides of the barrier and using Eq. (8) leads then to the relation

$$T^\dagger V T + \mathcal{R}^\dagger (-\tilde{V}) \mathcal{R} = V - \mathcal{R}^\dagger \gamma^\dagger + \gamma \mathcal{R}, \quad (9)$$

$$\mathcal{R} = Q_{22}^{-1} Q_{21}, \quad (10)$$

$$T = Q_{11} - Q_{12} Q_{22}^{-1} Q_{21}, \quad (11)$$

where $n_b \times n_b$ matrix Q is related to the transfer matrix T_{barr} of the $M+1$ -cell barrier beginning at site L :

$$Q = S_T^{-1} T_{barr} S_T = \begin{pmatrix} Q_{11} & Q_{12} \\ Q_{21} & Q_{22} \end{pmatrix},$$

$$\text{where } T_{barr} = T_{L+M} \cdots T_{L+1} T_L. \quad (12)$$

From now on we restrict ourselves to real T matrices (magnetic field is zero). In this case $\tilde{V} = -V$ (Ref. 15).

Besides the propagating waves, which correspond to complex eigenvalues of T with unit moduli, Eq. (9) includes the solutions decaying exponentially with distance from the barrier. Far from the barrier, the decaying solutions are not important. We reduce matrices \mathcal{T} , \mathcal{R} , and V , by removing rows

and columns corresponding to indices related to the decaying solutions. From Eq. (9) we obtain then the equation for the reduced matrices $\mathcal{T}_r, \mathcal{R}_r, V_r$:

$$\mathcal{T}_r^\dagger V_r \mathcal{T}_r + \mathcal{R}_r^\dagger V_r \mathcal{R}_r = V_r. \quad (13)$$

Equation (13) can be rewritten in the convenient form

$$\tau^\dagger \tau + \rho^\dagger \rho = I, \quad \tau = v \mathcal{T}_r v^{-1}, \quad \rho = v \mathcal{R}_r v^{-1} \quad (14)$$

and v is defined by the relation $v^\dagger v = V_r$.¹⁷ Equation (14) is a multichannel reflection law. In our calculation of the reflection matrix we use Eq. (14) as a test of the accuracy of the numerical computations. In order to obtain the explicit form of the reflection and transmission matrices we have to solve the eigenproblem for the transfer matrix for a specific model Hamiltonian—this is done in the next subsections.

A. Armchair nanotube

In an (N_a, N_a) armchair nanotube, a unit cell can be formed with $2N_a$ hexagons going round the tube. Carbon atoms in each cell belong to either of two planes perpendicular to the nanotube axis, a and b (see Fig. 1). In our nearest-neighbor (NN) hopping model the following hopping processes, all described by the same hopping parameter $t \sim 3.1$ eV (from now on treated as our energy unit), are possible: (a) $(a, m, 2\nu - 1) \leftrightarrow (a, m, 2\nu)$, (b) $(b, m, 2\nu) \leftrightarrow (b, m, 2\nu + 1)$, (c) $(a, m, \nu) \leftrightarrow (b, m, \nu)$, (d) $(a, m, \nu) \leftrightarrow (b, m - 1, \nu)$, where m denotes the unit-cell index and ν numbers consecutively the atoms we meet going round the a or b plane (the spin index will be omitted here). Also the proper periodic boundary conditions for ν are implied.

In the case of the diagonal disorder, to which we restrict ourselves in this subsection, the transfer matrix is given by Eq. (5) with $W_j = t_j = I$ and

$$A_m = \mathcal{L}^\alpha - I\omega + \Delta_m^a, \quad (\Delta_m^a)_{\mu\nu} = \delta_{\mu\nu} E_{m\nu}^a, \quad (15)$$

$$B_m = \mathcal{L}^\beta - I\omega + \Delta_m^b, \quad (\Delta_m^b)_{\mu\nu} = \delta_{\mu\nu} E_{m\nu}^b, \quad (16)$$

where $E_{m\nu}^{a,b}$ represent the site energy for the corresponding atoms, and matrices \mathcal{L} are:

$$\mathcal{L}_{\mu\nu}^\alpha = \begin{cases} \delta_{\mu, \nu+1} & \text{if } \mu \text{ even} \\ \delta_{\mu, \nu-1} & \text{if } \mu \text{ odd} \end{cases} \quad (1 \leq \mu \leq n_b/2), \quad (17)$$

$$\mathcal{L}_{\mu\nu}^\beta = \begin{cases} \delta_{\mu, \nu+1} & \text{if } \mu \text{ odd} \\ \delta_{\mu, \nu-1} & \text{if } \mu \text{ even} \end{cases} \quad (1 < \mu < n_b/2),$$

$$\mathcal{L}_{\mu(1/2)n_b}^\beta = \mathcal{L}_{(1/2)n_b, \mu}^\beta = \delta_{\mu 1} \quad (1 \leq \mu \leq n_b/2), \quad (18)$$

where $n_b = 4N_a$ is a total number of all atoms in the unit cell. The eigenequation for the transfer matrix of the perfect lattice site T

$$\begin{pmatrix} BA - I & B \\ -A & -I \end{pmatrix} \begin{pmatrix} x \\ y \end{pmatrix} = \lambda \begin{pmatrix} x \\ y \end{pmatrix}, \quad (19)$$

where x, y are $n_b/2$ -dimensional vectors, can be reduced to the eigenvalue problem for the vector x

$$BAx = \Omega x, \quad \Omega = \frac{(\lambda + 1)^2}{\lambda}, \quad y = -\frac{1}{1 + \lambda} Ax. \quad (20)$$

From Eqs. (15) and (16) we obtain the system of equations for the components of x

$$\begin{aligned} \frac{[1 - (-1)^\nu]}{2} x_{\nu-2} - \omega x_{\nu-1} - (\Omega - \omega^2) x_\nu - \omega x_{\nu+1} \\ + \frac{[1 + (-1)^\nu]}{2} x_{\nu+2} = 0, \end{aligned} \quad (21)$$

which has to be solved with respect to a boundary condition: $x_\nu = x_{\nu+n_b/2}$ determining q . The solution is given by

$$x_\nu = \left\{ \frac{a}{2} [1 - (-1)^\nu] + \frac{b}{2} [1 + (-1)^\nu] \right\} \exp(i\nu q), \quad (22)$$

$$\Omega = \omega^2 + \cos(2q) \pm \sqrt{\cos^2(2q) + 4\omega^2 \cos^2 q - 1}. \quad (23)$$

The matrix diagonalizing T with a similarity transformation is

$$S_T = \begin{pmatrix} S & S \\ -AS(1 + \Lambda)^{-1} & -AS(1 + \bar{\Lambda})^{-1} \end{pmatrix}, \quad (24)$$

where S is built of eigenvectors of BA and Λ denotes the diagonal matrix of the eigenvalues λ .

From the relation between Ω and λ [Eq. (20)] and the requirement that λ be a complex number of a modulus 1 ($\lambda = e^{ik}$, where k is real) the band energy can be calculated as

$$\omega_k^{\pm \pm'} = \pm \sqrt{3 + 2 \cos(k) \pm' 4 \cos q \cos(k/2)} \quad (25)$$

[$q = (\pi/n_b) m, m = 0, 1, \dots, n_b/2$] which agrees with the results obtained in an earlier work.¹⁸

B. Zigzag nanotube

In the case of zigzag-type nanotube $(N_a, 0)$ the unit cell of 1D lattice can be defined as a belt of N_a complete octahedra touching side by side and going round the tube. In such a choice of the unit cell (see Fig. 1), some atoms (a and b type) connect atoms from neighboring cells while others (z and h) are connected to the atoms from the same cell only.

By elimination of ‘‘internal’’ components, we arrive at system of equations relating α and β only at the cost of appearance of the ω -dependent intracell hopping W_m . In this case $t_m = I$, $n_b = 2N_a$, and

$$A_m = \mathcal{L}^T (1 - Z_m H_m)^{-1} H_m \mathcal{L} - I\omega + \Delta_m^a, \quad (26)$$

$$B_m = \mathcal{L}^T (1 - Z_m H_m)^{-1} Z_m \mathcal{L} - I\omega + \Delta_m^b, \quad (27)$$

where $Z_{m, \mu\nu} = \delta_{\mu\nu} (E_{m\nu}^z - \omega)$, $H_{m, \mu\nu} = \delta_{\mu\nu} (E_{m\nu}^h - \omega)$,

$$\mathcal{L}_{\mu\nu} = \begin{cases} \delta_{\mu\nu} + \delta_{\mu, \nu-1} & \text{for } \mu < n_b/2 \\ \delta_{\nu 1} + \delta_{\nu, n_b/2} & \text{for } \mu = n_b/2. \end{cases} \quad (28)$$

The effective intracell hopping operator W_m reads

$$W_m = -\mathcal{L}^T (1 - Z_m H_m)^{-1} \mathcal{L}. \quad (29)$$

The eigenequation for T can be solved in similar way as for the case of the armchair nanotube, if we note that the operators A , B , and W now commute and can be simultaneously diagonalized. The similarity transformation that diagonalizes T is represented by the matrix

$$S_T = \begin{pmatrix} S & S \\ -AS + W^2A^{-1}S + WA^{-1}S\Lambda & -AS + W^2A^{-1}S + WA^{-1}S\bar{\Lambda} \end{pmatrix}, \quad S_{\mu\nu} = \frac{e^{i\mu q_\nu}}{\sqrt{n_b/2}}. \quad (30)$$

Here we note that the present formulation requires the reversibility of the effective transfer matrix W . However, W is not reversible for the nanotubes $(N_a, 0)$ with N_a even. The problem can be traced back to the existence of a dispersionless bands at $\omega = \pm 1$ for these tubes. It can be easily remedied by first applying the similarity transformation defined by the matrix S to the recurrence relations, Eqs. (3) and (4). Then a $(N_a/2)$ th row and $N_a/2$ column of the transformed matrices $S^\dagger W_m S$ will be composed of zeros only. As a result, two coupled equations for the $(N_a/2)$ th components of the vectors $S^\dagger \alpha_m, S^\dagger \beta_{m-1}$

$$(E_{m, N_a/2}^\alpha - \omega)(S^\dagger \alpha_m)_{N_a/2} + (S^\dagger \beta_{m-1})_{N_a/2} = 0, \quad (31)$$

$$(E_{m-1, N_a/2}^\beta - \omega)(S^\dagger \beta_{m-1})_{N_a/2} + (S^\dagger \alpha_m)_{N_a/2} = 0 \quad (32)$$

will have nonzero solutions only if $\omega = \pm 1$. We can thus apply the formalism presented above for a reduced system of variables with reversible reduced matrices $S^\dagger A_m S$, $S^\dagger B_m S$, and $S^\dagger W_m S$ obtained from the original ones by removing the $(N_a/2)$ th columns and rows.

The eigenvalues of T are

$$\lambda_\nu^\pm = \frac{1}{2} \left(\frac{A_\nu^2}{W_\nu} - \frac{1}{W_\nu} - W_\nu \right) \pm \sqrt{\left[\frac{1}{2} \left(\frac{A_\nu^2}{W_\nu} - \frac{1}{W_\nu} - W_\nu \right) \right]^2 - 1} \quad \left(\nu \neq \frac{N_a}{2} \right), \quad (33)$$

where A_ν and W_ν are eigenvalues of A and W , respectively,

$$W_\nu = -\frac{4 \cos^2(q_\nu/2)}{1 - \omega^2}, \quad A_\nu = \omega(W_\nu - 1) \quad (34)$$

and $q_\nu = 4(\pi/n_b)\nu, \nu = 1, \dots, n_b/2$. The band energy is obtained from the equation

$$\frac{1}{2} \left(\frac{A_\nu^2}{W_\nu} - \frac{1}{W_\nu} - W_\nu \right) = \cos(k) \quad (35)$$

solution of which is

$$\omega_k^{\pm \pm'} = \pm \sqrt{1 + 4 \cos^2(q_\nu/2) \pm' 4 \cos(q_\nu/2) \cos(k/2)}. \quad (36)$$

This result again agrees with that of earlier works.¹⁸

III. RESULTS AND DISCUSSION

The first part of our computations concerned a simple pointlike defect and these results provide a reference point to

discuss more complex and more realistic defects in SWCNT. The pointlike defect is defined by setting site energy equal to E at one of the sites of the unit cell, with all the other sites having site energy zero. We have computed a reflection coefficient R defined as

$$R = \text{Tr}(\rho^\dagger \rho) / n_c,$$

where n_c is the number of conducting channels. This has been done for both armchair and zigzag nanotubes varying nanotubes' radii and the strength of the point defect E . The reflection coefficient can be simply related to a conductance:¹⁴

$$\Gamma = \frac{e^2}{2\pi\hbar} \text{Tr}(\tau^\dagger \tau)$$

by a sum rule following from Eq. (14): the value of $1 - R$ can be interpreted as a conductance (in units of $e^2/2\pi\hbar$) per conducting channel.

In Fig. 2, we present evolution of the ω -dependence of the reflection coefficient R with a strength of defect E for the armchair (2,2) nanotube. For small value of E , $E \ll 1$ (we recall that $t = 3.1$ eV is our energy unit here) the reflection R shows a behavior closely resembling the one of the density of states (DOS) for the same nanotube (Fig. 3). This is similar to what we find in the single-band tight-binding model, where reflection from a single defect is given by

$$R_1 = \frac{(E/2t)^2}{(E/2t)^2 + 1 - (\omega/2t)^2}.$$

With increase of the defect strength the reflection grows initially as E^2 and the peaks in ω dependence become more smooth. At the same time, the overall picture becomes more asymmetric with respect to $\omega = 0$. The latter, unlike in a single-band case, may have important consequences also for other transport properties of the system, such as the thermoelectric power (TEP). The Seebeck coefficient, as calculated from a Boltzmann kinetic theory with a relaxation time symmetric in ω would identically vanish for the half-filled band case for the symmetric band structure that we have in SWCNT in the nearest-neighbor hopping model. On the other hand, the measured values of TEP gives quite a sizable linear-in-temperature dependence,¹⁹ suggesting some mechanism that breaks the electron hole symmetry.

For large enough E , $E > 1$, we find that the peak which for small E is located at $\omega = -1$ smoothes and moves towards higher values of ω as E increases. This behavior of R suggests appearance of a resonance state.

We examined how the changes of $R(\omega)$ with E are compared with the spectral density. We calculated the change in

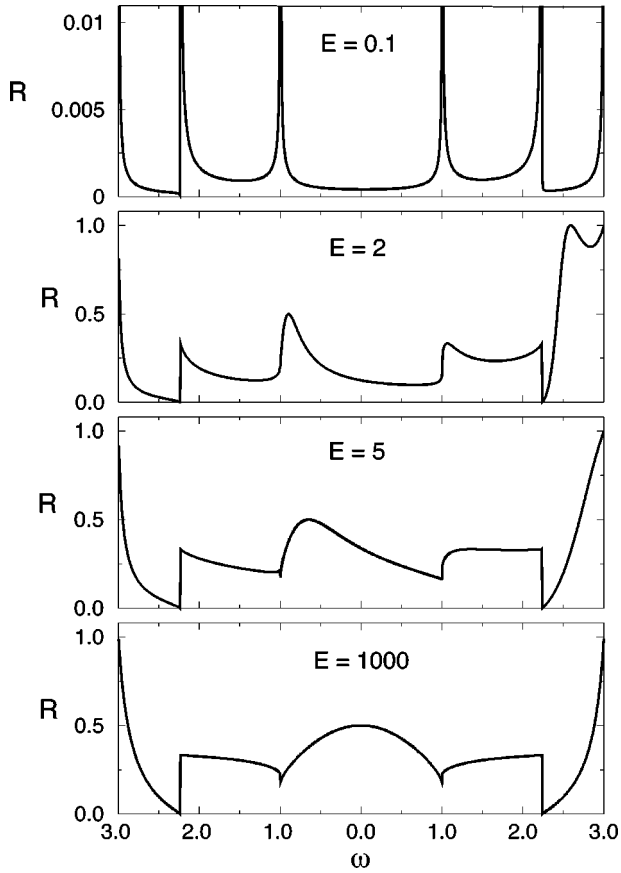


FIG. 2. Change of a reflection from a point defect in an armchair (2,2) nanotube with defect strengths: $E=0.1, 2, 5, 1000$. The sharp peaks seen for $E=0.1$ can be matched to the ones in a density of states for the same nanotube. The broad maximum, which begins to emerge for $E>2$ and is centered close to $\omega=0$ for strong E and suggests appearance of a resonant state.

DOS, $\Delta\rho$, due to the introduction of the defect (see the Appendix). A typical behavior of $\Delta\rho$ is shown in Fig. 4 for $E=2$ and (2,2) nanotube. A small resonance peak is observed in the region of $\sqrt{5}<\omega<3$ for $0.5<E<3$, corresponding to the highest nondegenerate band. For $E\rightarrow 3$ the peak shifts to the highest band edge and appears to hybridize with an undamped localized state existing for $\omega>3$. The localized state then departs from the band system and travels fast away from it with a further increase of E . The resonance peak may be interpreted as a quasilocalized state of the system. It occurs in the frequency region where the density of states (and

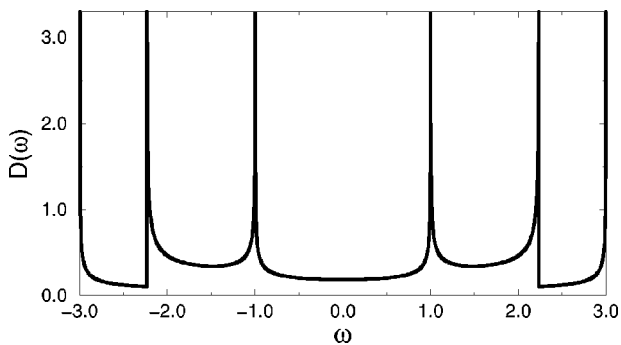


FIG. 3. The density of states of (2,2) nanotube.

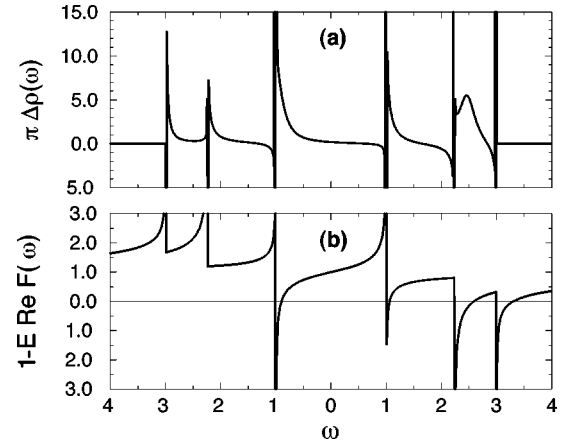


FIG. 4. Change of DOS, $\pi\Delta\rho$ due to a point defect in the (2,2) nanotube for $E=2$ (a) and a real part of the denominator of $\pi\Delta\rho$, $\text{Re}[1-EF(\omega)]$ (b). Zeros of $1-E\text{Re}F(\omega)$ determine energy of resonance solutions (the one most clearly seen here is for $\omega\approx 2.6$) and a localized solution outside the band system at $\omega\approx 3.30$ [its δ -like peak in (a) was not shown here].

hence the damping) is relatively small. The same peak is seen in R in Fig. 2, where for $E=2$, $R=1$ at its maximum. The maximum observed in R for $-1<\omega<1$ is not seen directly in behavior of $\Delta\rho$ for $N_a=2$ due to a relatively large unperturbed DOS. It is however observed for $N_a\geq 3$, since the DOS near $\omega=0$ decreases with increase of N_a .

The condition for the appearance of the resonant or localized solutions are given by zeros of the real part of denominator of $\Delta\rho$, $1-E\text{Re}F(\omega)$ [see Eq. (A7)]. In this case, the zero matches the position of the maximum in R (where $R=1/2$) in the range $-1<\omega<1$ (Fig. 4). The position of the zero approaches $\omega=0$ for a very strong E . One might then interpret the round maximum of R near $\omega=0$ in Fig. 2 for large E as related to strongly overdamped resonance in this case originating entirely from the middle bands with $\varepsilon_k = \pm\sqrt{1+4\cos^2 k/2}$. Contributions for $\text{Re}F(\omega)$ from the remaining bands exactly cancel out in the $-1<\omega<1$ region. An analogous relation between zeros of $1-E\text{Re}F(\omega)$ and position of maximum of R is observed for $1<\omega<\sqrt{5}$ with $R=1/3$ in its maximum.

The value of the reflection coefficient at the points of resonance can be understood as follows. Suppose ω_0 is the exact eigenvalue of the Hamiltonian \mathcal{H} and satisfies $1-E\text{Re}F(\omega_0)=0$. Furthermore, assume that $\varepsilon_0 = \varepsilon_{k_1,1} = \dots = \varepsilon_{k_g,g} = \omega_0 + O(1/N)$, where ε_0 is the eigenvalue of the Hamiltonian with no defect \mathcal{H}_0 with degeneracy g (we consider running waves only), ν is the band index, and N is the number of unit cells in the system. Then one can find $g-1$ independent linear combinations of the eigenstates of \mathcal{H}_0 , $\phi_{k_\nu,\nu}$, $\nu=1, \dots, g$, of the form $\psi_\mu = \sum_{\nu=1, \dots, g} \alpha_{\mu\nu} \phi_{k_\nu,\nu}$, with a property that: $\mathcal{H}\psi_\mu = \varepsilon_0\psi_\mu$ and $\mathcal{H}_1\psi_\mu = 0$ [\mathcal{H}_1 is a Hamiltonian of the point defect, see Eqs. (A1) and (A2)]. These states will not scatter from the defect and contributions from them to $\text{Tr}(\rho^\dagger\rho)$ will vanish. A wave corresponding to a resonant (or quasilocalized) solution, orthogonal to states ψ_μ , will be perfectly reflected and contribute 1 to $\text{Tr}(\rho^\dagger\rho)$. As a result the reflection coefficient at the energy of a resonance will be equal to $1/n_c$ and have a local maximum

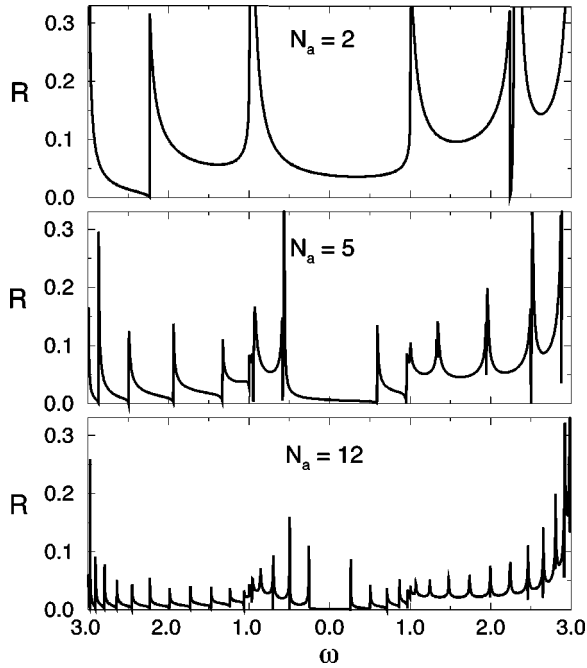


FIG. 5. Reflection from a point defect of strength $E=1$ for several armchair (N_a, N_a) nanotubes, $N_a=2,5,12$. Note deepening of the transmission window present around $\omega=0$ with increase of the nanotube radius.

at this point. This property seems to hold to a good approximation also for any defect of extension much smaller than the nanotube radius as can be exemplified by the 5-77-5 defect for large enough N_a (see below and Fig. 9).

The evolution of the ω dependence of the reflection with the diameter for $E=1$ is presented for armchair and zigzag nanotubes in Figs. 5 and 6, respectively. One can see a deepening of the transmission window around $\omega=0$ with increase of N_a and a relatively slow decrease of R in the rest of ω range.

In order to make a more general conclusion concerning dependence of the reflection coefficient on N_a and E , we plotted the reflection coefficient calculated for $\omega=0$ as a function of N_a for several values of E in the log-log scale in the Fig. 7. The curves obtained for weak E values show that R scales like

$$R \sim s \frac{E^2}{N_a^2} \quad (37)$$

with $s \approx 1/6$ and $s \approx 1/2$ for the armchair and zigzag nanotubes, respectively. This scaling holds in the case of larger defect strength as well, but then one has to go to larger values of N_a to see it.

Besides the value of the reflection at $\omega=0$, it is of interest to see the asymmetry in the ω dependence around this point. As follows from Fig. 8, the relative asymmetry increases with increase of the nanotube radius.

Many features of the behavior of reflectance can be understood using an analogy with the simpler case described in Ref. 15 where we have orbitals of only one kind in the unit cell. For the case of diagonal disorder only ($t_n = I$), the similarity transformation, which diagonalizes the transfer matrix T can be obtained as

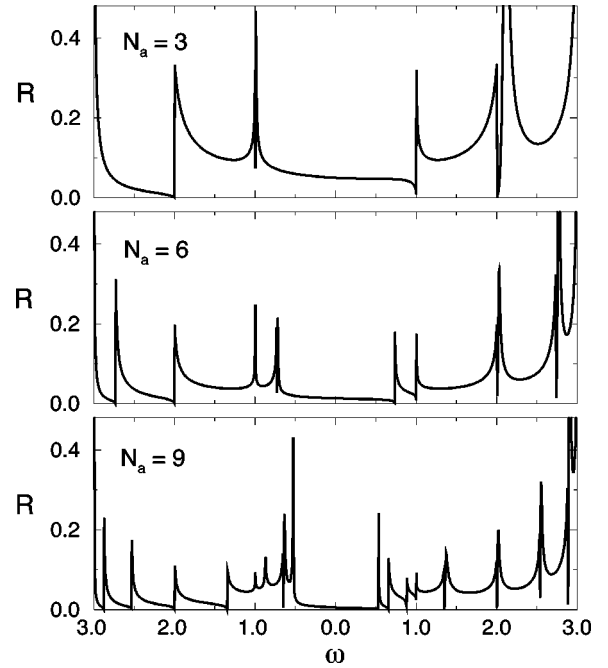


FIG. 6. The same as in Fig. 5 for several zigzag $(N_a, 0)$ nanotubes, $N_a=3,6,9$.

$$S_T = \begin{pmatrix} S & S \\ S\Lambda & S\tilde{\Lambda} \end{pmatrix}, \quad (38)$$

where S is made of eigenvectors of the matrix H . Then, the velocity matrix $V = \Lambda - \tilde{\Lambda}$. One can write the explicit expression for the reflection matrix \mathcal{R}

$$\mathcal{R} = -(I-x)^{-1}x, \quad x = V^{-1}S^\dagger(T-T_{barr})S \quad (39)$$

For a small defect strength, the denominator in Eq. (39) may be neglected. In this case, rapid changes of R near the van Hove singularities in DOS are due to the prefactor V^{-1} , which is the inverse of the group velocity for relevant bands.

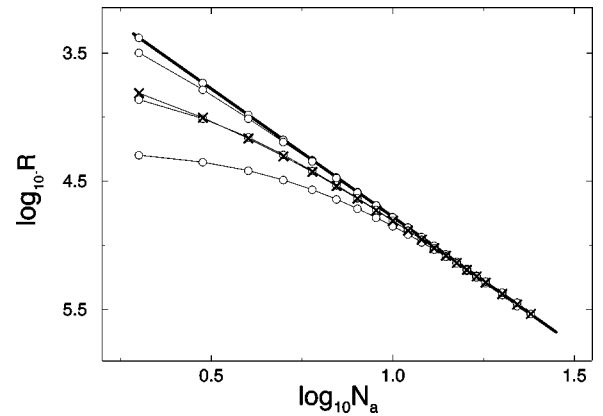


FIG. 7. Scaling of the reflection at $\omega=0$ with the parameter N_a of the armchair (N_a, N_a) nanotube for several values of the point defect strength: $E=0.1,2,5,10$. The sets of data for various E were scaled so that to have a common point for $(24,24)$ nanotube. The bigger is the defect strength, the later the scaling behavior is seen. Crosses show R vs N_a dependence for the 5-77-5 defect: note a close similarity to a point defect with $E=5$. The heavy line gives $1/N_a^2$ dependence.

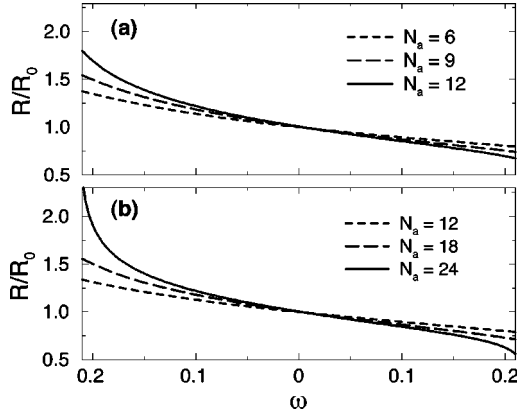


FIG. 8. Scaled according to the $1/N_a^2$ dependence reflection from a single-point defect as a function of ω in vicinity of $\omega=0$ for several (N_a, N_a) armchair ($N_a=6,9,12$) (a) and zigzag ($N_a, 0$) ($N_a=12,18,24$) (b) nanotubes, for the same defect strength $E=1$. The reflection becomes more asymmetric with increase of N_a .

It diverges at the band edges [of course x in the denominator of Eq. (39) becomes also important very close to this point]. In this way we can explain the qualitative similarity of Figs. 3 and 2(a). The $1/N_a^2$ scaling is related to normalization $1/\sqrt{N_a}$ prefactors present in eigenfunctions of \mathcal{H}_0 [compare this to S in Eq. (30)]. Note however that this scaling behavior will be seen near $\omega=0$ as long as we can neglect rapid changes in the denominator of \mathcal{R} in the vicinity of band edges.

The scaling behavior can be understood by considering low-electron excitations near $\omega=0$ (i.e., half-filled band). Independent on the nanotube radius, there are only two bands which intersect the Fermi surface. It is therefore possible to disregard (“project out”,²⁰) the other bands, provided that the defect strength is small enough ($E \ll 1$). In this case, the initial Hamiltonian can be reduced to a two-band model with distance dependent hopping and an on-site point defect of an effective strength $\tilde{E}=E/4N_a$ (see the Appendix for details). With a change of the nanotube radius, only the effective defect strength changes, while the hopping integrals do not depend on N_a . For small enough \tilde{E} the reflectivity will go like square of a defect strength, because $R = \text{Tr}(\rho^\dagger \rho)/n_c$ (with $\rho \sim T - T_{barr} \sim \tilde{E}$) while $n_c=2$ for any N_a . This gives rise to the $1/N_a^2$ dependence of R .

As the defect strength becomes larger, x increases and the effects of the band structure in R are less pronounced (see Fig. 2 for $E=1000$), because the numerator and the denominator in Eq. (39) are comparable. In this region of E , we obtained a very good quantitative agreement with the results of Ref. 8, showing a relatively smooth and symmetric with respect to $\omega=0$ dependence of the conductance for (4,4) nanotube with a vacancy.

The point defect discussed so far can be considered as a very simplified model of more realistic defects present in the graphene sheet. The systematic study of various possible defects in the SWCNT (see, e.g., Refs. 4 and 6) is beyond the scope of the present paper. Instead we restrict ourselves to so called 5-7-7-5 defect in an armchair nanotube. This defect can be obtained by rotating one of the C-C bonds by $\pi/2$ resulting in the transformation of four of nearby hexagons into a

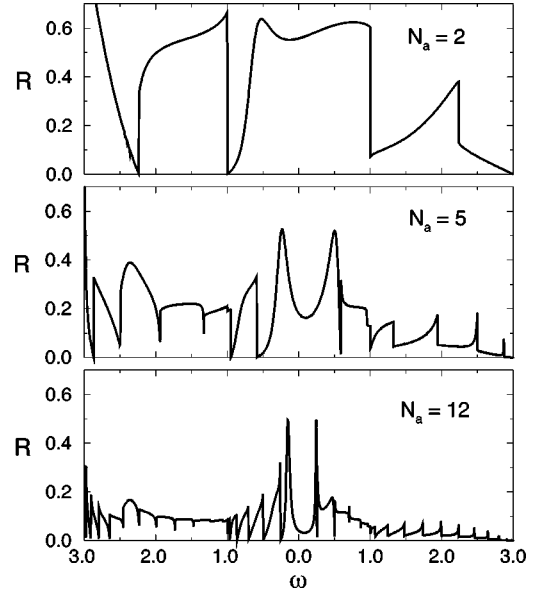


FIG. 9. The reflection from the 5-7-7-5 defect shown as a function of ω for armchair nanotubes (2,2), (5,5), (12,12). This is to be compared to Fig. 5, where the corresponding data for a single point defect are shown.

pair of heptagons having a common side and separating two pentagons (see Fig. 1). It can be modeled by considering the hopping matrices in the form shown below for the (2,2) nanotube

$$t_L = \begin{pmatrix} 1 & 0 & 0 & 0 \\ 0 & y & 1-y & 0 \\ 0 & 0 & 1 & 0 \\ 0 & 0 & 0 & 1 \end{pmatrix}, \quad W_L = \begin{pmatrix} 1 & 0 & 0 & 0 \\ 0 & 1 & 0 & 0 \\ 0 & 1-y & y & 0 \\ 0 & 0 & 0 & 1 \end{pmatrix}. \quad (40)$$

In this case the barrier matrix is made of a product of the two consecutive transfer matrices: $T_{barr} = T_{L+1} T_L$ [see Eq. (5)]. The parameter y that appears in Eq. (40) allows us to study the defect systematically starting from a perfect lattice for $y=1$, and approaching 5-7-7-5 defect for $y=0$. Note that for $y=0$ the matrices t_L and W_L are not reversible (this would not be the case if we went beyond the nearest-neighbors hopping in our model). We solve this problem by approaching $y=0$ by interpolation made from several values of y close to zero. This can be easily done, as $R(y)$ is a quite smooth function of y [the accuracy of computations in this approach is checked using Eq. (14)].

The details of the ω dependence of the reflection coefficient for the 5-7-7-5 defect show some similarities with those for point defects with a very high value of E . In fact, we found the same scaling ($R \sim 6/N_a^2$) with N_a as in the case of the point defect with energy $E \approx 6$. This latter value is equal to a total bandwidth and can be qualitatively understood as follows. In the presence of 5-7-7-5 defect, as shown in the Fig. 1, the number of links between two consecutive unit cells is reduced by one. The same effect can be achieved by placing a strong defect (comparable to a bandwidth) in one lattice site, and effectively blocking the link joining this site.

The value of the reflection at $\omega=0$ for the 5-7-7-5 defect for the (10,10) armchair nanotube is rather sizable: R

≈ 0.056 . Knowing this value one can roughly estimate the upper limit for a concentration of these defects from a conductance measurements. Assuming that R is small enough that we can neglect backscattering the total transmission of a chain having p defects of this type may be estimated as $T_p = (1-R)^p$. For instance, for a transmission $T_p = 1/60$, as in Ref. 3 (note however that the last estimate included unknown contribution from a contact resistance), and the nanotube length $3 \mu\text{m}$, one finds that the average distance between these defects is not less than $\approx 40 \text{ nm}$.

In conclusion, we present a formalism suitable to be applied for the calculations of the influence of defects on the residual conductivity of carbon nanotubes, and used it to calculate reflection of simple defects. The calculations were based on the tight-binding model, with no electron-electron interactions, since we concentrated our attention on the effects of the one-electron band structure. The disregard of the electron correlations may be seen as an important restriction of the validity of the present calculation in the light of the results obtained for the one channel case using the Luttinger model.²¹ Although theory suggests nanotubes are Luttinger liquids, experiments indicate they are Fermi liquids.

It would be interesting to see what are the effects of interactions on R in the present multichannel case. A perturbative renorm-group calculation²² for the two-band case show that the dominating correlations for the half-filled band case may be either spin-density wave or charge-density wave, in the former case possibly invalidating the predictions based on the Luttinger model. Other conclusions, based on the exact calculation of the Kubo conductivity at $T=0 \text{ K}$ were obtained for a model of interacting electrons with disorder on a small 2D cylinder. These results suggest that the conductivity may be weakly dependent on the interaction in the weak interaction limit.²⁴ One cannot tell for sure yet to what extent this weak interaction limit is relevant for SWCNT.

On the experimental side, there are few indications of any drastic effect of correlations on the transport properties. A magnetoresistance measurement suggests the localization of electronic states rather than electron correlations are responsible for the increase of resistivity for $T \rightarrow 0 \text{ K}$ (Ref. 23) in multiwalled nanotubes. It would be of interest to extend the above calculations for a finite concentration of defects to see what influence they may have on density of states close to the Fermi level as well as on the localization of electronic wave functions.

ACKNOWLEDGMENTS

The authors are grateful to B. Bułka, R. Micnas, and R. Buczko for their critical comments. Research support is acknowledged from the University of Tennessee, from Oak Ridge National Laboratory managed by Lockheed Martin Energy Research Corp. for the U.S. Department of Energy under Contract No. DE-AC05-96OR22464, and from Research Grant No. N00014-97-1-0565 from the Applied Research Projects Agency managed by the Office of Naval Research. T.K. and M.B. also acknowledge support from the Committee of Scientific Research (K.B.N Poland), Project Nos. 2 P03B 056 14 and 2P03B 104 11. This research was supported in part by the Oak Ridge National Laboratory and the Oak Ridge Institute for Science and Education.

APPENDIX A: CHANGE IN DOS DUE TO A POINT DEFECT

In this appendix we calculate a change in density of states in an armchair nanotube (N_a, N_a), due to introduction of a single-point defect. The Hamiltonian of the system including a single defect in a position L of otherwise perfect lattice can be written in k -space representation as

$$\mathcal{H} = \mathcal{H}_0 + \mathcal{H}_1 = \sum_k \begin{pmatrix} a_k^\dagger & b_k^\dagger \end{pmatrix} \begin{pmatrix} H^a & te^{-ik} + W \\ te^{ik} + W & H^b \end{pmatrix} \begin{pmatrix} a_k \\ b_k \end{pmatrix} + \frac{1}{N} \sum_{k,k'} \begin{pmatrix} a_k^\dagger & b_k^\dagger \end{pmatrix} \begin{pmatrix} \Delta^a & 0 \\ 0 & \Delta^b \end{pmatrix} \begin{pmatrix} a_{k'} \\ b_{k'} \end{pmatrix} e^{i(k'-k)L}, \quad (\text{A1})$$

where Δ^a, Δ^b define potential of the impurity, N is the number of unit cells, $H^a = \mathcal{L}^\alpha$, $H^b = \mathcal{L}^\beta$. Introducing a representation diagonalizing \mathcal{H}_0 , Eq. (A1) can be rewritten as

$$\mathcal{H} = \sum_{k\mu} \varepsilon_{k\mu} c_{k\mu}^\dagger c_{k\mu} + \frac{E}{N} \sum_{kk'\mu\nu} e^{i(k'-k)L} f^*(k)_{\delta\mu} f(k')_{\delta\nu} c_{k\mu}^\dagger c_{k'\nu}, \quad (\text{A2})$$

where μ, ν are band indices,

$$\varepsilon_{k\nu} = \sqrt{[\cos(\pi\nu/N_a) + 2\cos(k/2)]^2 + \sin^2(\pi\nu/N_a)}$$

for $\nu = 1, \dots, 2N_a$ and $\varepsilon_{k\nu} = -\varepsilon_{k\nu-2N_a}$ for $\nu > 2N_a$. $\delta = 1, \dots, 4N_a$ refers to a position of a defect of a strength E in the L th unit cell, and c_k is a $4N_a$ -dimensional annihilation operator. Coefficient $f(k)_{\nu\mu}$ is an element of a matrix of a unitary transformation, which reduces \mathcal{H}_0 to a diagonal form:

$$f(k) = \begin{pmatrix} S & S \\ Se^{ik/2} & -Se^{ik/2} \end{pmatrix} \begin{pmatrix} I & \mathbf{0} \\ \mathbf{0} & \begin{pmatrix} \mathbf{0} & I \\ I & \mathbf{0} \end{pmatrix} \end{pmatrix} \times \begin{pmatrix} \alpha(k+) & \alpha(k-) \\ \beta(k+) & \beta(k-) \end{pmatrix}, \quad S_{\mu\nu} = \frac{1}{\sqrt{4N_a}} e^{i\pi\mu\nu/N_a}, \quad (\text{A3})$$

where elements of the diagonal $2N_a \times 2N_a$ matrices α, β read

$$\beta(k\sigma)_{\nu\nu} = -i\alpha(k\sigma)_{\nu\nu} \frac{\left(\sigma |\varepsilon_{k\nu}| - \cos \frac{\pi\nu}{N_a} - 2 \cos \frac{k}{2} \right)}{\sin \frac{\pi\nu}{N_a}},$$

$$|\alpha(k\sigma)_{\nu\nu}|^2 + |\beta(k\sigma)_{\nu\nu}|^2 = 1,$$

$$\alpha(k+)_{\nu N_a} = \beta(k-)_{\nu N_a} = \delta_{\nu N_a},$$

$$\alpha(k-)_{\nu N_a} = \beta(k+)_{\nu N_a} = 0. \quad (\text{A4})$$

For small-enough defect strength ($E \ll 1$), and as long as low-energy excitations are concerned, one can skip all bands in Eq. (A1), except the ones with indices $\nu = N_a, 3N_a$ that intersect the Fermi surface. In this case,

$$\begin{aligned} f(k)_{\delta,\nu}^* f(k')_{\delta,\nu} &= 1/4N_a, f(k)_{\delta,N_a}^* f(k')_{\delta,3N_a} = \pm 1/4N_a, \varepsilon_{k N_a} \\ &= 1 - 2 \cos(k/2), \\ \varepsilon_{k 3N_a} &= -1 + 2 \cos(k/2) \end{aligned}$$

The Hamiltonian, when transformed back to the real space, takes the form of a two-band model with on site point defect of the effective strength $E/4N_a$ and a hopping that depends on distance:

$$\begin{aligned} \mathcal{H} &= \sum_{m,j; \mu=N_a, 3N_a} t_{j,j+m}^{(\mu)} (c_{j\mu}^\dagger c_{j+m,\mu} + \text{H.c.}) \\ &+ \frac{E}{4N_a} \sum_{\mu\nu=N_a, 3N_a} c_{L\mu}^\dagger c_{L\nu}, \end{aligned} \quad (\text{A5})$$

where

$$\begin{aligned} t_{j,j+m}^{(N_a)} &= \delta_{m,0} + \frac{(-1)^m}{N} \frac{\sin\left(\frac{\pi}{N}\right)}{\sin\left[\frac{\pi}{N}\left(m + \frac{1}{2}\right)\right] \sin\left[\frac{\pi}{N}\left(m - \frac{1}{2}\right)\right]} \\ &\sim \delta_{m,0} + \frac{(-1)^m}{\pi(m^2 - 1/4)} \end{aligned} \quad (\text{A6})$$

and $t_{j,j+m}^{(3N_a)} = -t_{j,j+m}^{(N_a)}$. Note that the prefactor $1/N_a$ in the effective defect strength comes entirely from the normalization of the electronic wave functions of \mathcal{H}_0 and measures the proportion of electron density in the considered state residing on the defect site.

One can easily calculate the change of density of states due to the point defect using the Green's function method (see, e.g., Ref. 25). The result is

$$\begin{aligned} \pi \Delta \rho(\omega) &= E \text{Im} \frac{dF(\omega)}{1 - EF(\omega)}, \\ F(\omega) &= \frac{1}{N} \sum_{k\nu} \frac{|f(k)_{\delta\nu}|^2}{\omega + i0^+ - \varepsilon_{k\nu}} \end{aligned} \quad (\text{A7})$$

where one notes, using Eqs. (A3) and (A4), that $|f(k)_{\delta\nu}|^2 = 1/4N_a$.

-
- ¹M. S. Dresselhaus, G. Dresselhaus, and R. Saito, Carbon **33**, 883 (1995); J. W. Mintmire and C. T. White, *ibid.* **33**, 893 (1995); J.-P. Issi, L. Langer, J. Heremans, and C. H. Olk, *ibid.* **33**, 941 (1995).
- ²P. M. Ajayan and T. W. Ebbesen, Rep. Prog. Phys. **60**, 1025 (1997).
- ³S. J. Tans, M. H. Devoret, H. J. Dai, A. Thess, R. E. Smalley, L. J. Geerligs, and C. Dekker, Nature (London) **386**, 474 (1997).
- ⁴R. Saito, G. Dresselhaus, and M. S. Dresselhaus, Chem. Phys. Lett. **195**, 537 (1992).
- ⁵C. J. Brabec, A. Maiti, and J. Bernholc, Chem. Phys. Lett. **219**, 473 (1994).
- ⁶T. W. Ebbesen and T. Takada, Carbon **33**, 973 (1995).
- ⁷L. Chico, V. H. Crespi, L. X. Benedict, S. G. Louie, and M. L. Cohen, Phys. Rev. Lett. **76**, 971 (1996).
- ⁸L. Chico, L. X. Benedict, S. G. Louie, and M. L. Cohen, Phys. Rev. B **54**, 2600 (1996).
- ⁹P. Lambin, A. A. Lucas, and J. C. Charlier, J. Phys. Chem. Solids **58**, 1833 (1997).
- ¹⁰R. Tamura and M. Tsukada, Phys. Rev. B **55**, 4991 (1997); Z. Phys. D **40**, 432 (1997).
- ¹¹J. W. Mintmire, B. I. Dunlap, and C. T. White, Phys. Rev. Lett. **68**, 631 (1992).
- ¹²J. M. Ziman, *Models of Disorder* (Cambridge University Press, London, 1979).
- ¹³R. Landauer, Philos. Mag. **21**, 863 (1970).
- ¹⁴D. S. Fisher and P. A. Lee, Phys. Rev. B **23**, 6851 (1981).
- ¹⁵L. Molinari, J. Phys. A **30**, 983 (1997).
- ¹⁶B. Kramer and A. MacKinnon, Rep. Prog. Phys. **56**, 1469 (1993).
- ¹⁷Positive definiteness of V_r is assured by including into matrix Λ , eigenvalues of T , corresponding to running waves allowed behind the barrier.
- ¹⁸R. Saito, M. Fujita, G. Dresselhaus, and M. S. Dresselhaus, Phys. Rev. B **46**, 1804 (1992).
- ¹⁹J. Hone, I. Ellwood, M. Muno, A. Mizel, M. L. Cohen, A. Zettl, A. G. Rinzler, and R. E. Smalley, Phys. Rev. Lett. **80**, 1042 (1998).
- ²⁰C. T. White and T. N. Todorov, Nature (London) **393**, 240 (1998).
- ²¹C. L. Kane and M. P. A. Fisher, Phys. Rev. B **46**, 15 233 (1992); G. Gómez-Santos, Phys. Rev. Lett. **76**, 4223 (1996).
- ²²Yu A. Krotov, D.-H. Lee, and S. G. Louie, Phys. Rev. Lett. **78**, 4245 (1997).
- ²³L. Langer, V. Bayot, E. Grivei, J. P. Issi, J. P. Heremans, C. H. Olk, L. Stockman, C. Van Haesendonck, and Y. Bruynseraede, Phys. Rev. Lett. **76**, 479 (1996).
- ²⁴R. Berkovits and Y. Avishai, Phys. Rev. Lett. **76**, 291 (1996).
- ²⁵G. D. Mahan, *Many-Particle Physics* (Plenum Press, New York, 1990).